17th World Conference on Earthquake Engineering, 17WCEE
Sendai, Japan - September 13th to 18th 2020

DYNAMIC CENTRIFUGE MODEL TESTS ON SLOPES WITH WATER IN THE BASE REGION

J. Xu[(1)], R. Uzuoka[(2)], K. Ueda[(3)]

[(1)] *Ph. D Student, Department of Civil and Earth Resources Engineering, Kyoto University, xu.jiawei.38z@st.kyoto-u.ac.jp.*
[(2)] *Professor, Disaster Prevention Research Institute, Kyoto University, uzuoka.ryosuke.6z@kyoto-u.ac.jp.*
[(3)] *Assistant Professor, Disaster Prevention Research Institute, Kyoto University, ueda.kyohei.2v@kyoto-u.ac.jp.*

Abstract

Stability of slopes where water was accumulated at the toe area during dynamic events were studied in this paper. The soil below and right above water level tended to be loose due to water storage at the toe of slope, and the slope behavior became different compared with those without water storage in the base area. Several model tests in a geotechnical centrifuge were carried out in this paper to examine the effects of water accumulation at slope toe, relative density of soil, and shaking intensity of dynamic events on the slope stability. The compression of the soil below the water level and localized failure at the toe region acted as the main trigger to shear the soil above the water level. Because of widely existing high suctions in the upper part of the slopes, total collapse was not possible even in model where intense shaking was excited. Seepage and capillary flow are two factors that need further attention in the study of the dynamic response of slopes subjected to water storage at toe. Cracks were concentrated at areas near the water level. Increasing the shaking intensity or successive shaking on a slope with a certain height of water at its toe area will not produce total collapse of the slope unless more infiltration time is given before the shaking. A large landslide below certain height of the slope can be caused by a strong shaking and the cracks on the unsaturated part of the slope is deepened as the intensity of the shaking increases. The shaking in tests in this study was introduced right after designated centrifugal accelerations were achieved and the time for seepage and capillary rise was very limited. In future study, model tests with elongated time for these phenomena are needed.

Keywords: slope stability, water storage, dynamic response, unsaturated slopes

1. Introduction

Slope stability under earthquakes were widely studied and most of the related research were focused on the saturated slopes by means of different methods, such as physical model experiments or numerical computation. As to unsaturated slopes, the change of suction during shaking influences the strength of soil and thus the stability of slope, which differ themselves greatly from saturated slopes The fluctuation of reservoir water level imposes great risks to the stability of the slope and landslides are likely to take place in certain reservoir areas (Wang et al., 2007; Sun et al., 2016). Field monitoring methods (Fujita, 1977; Kilburn and Petley, 2003; Qi et al., 2006; Pinyol et al., 2012; Wang et al., 2014) were usually applied by a lot of researchers to predict the slope stability, and few physical experiments (Miao et al., 2016; Xiong et al., 2019) were carried out to simulate the real events or predict slope behaviors. However, these studies focused on the effects of the water level on the static stability of slopes and dynamic response of these slopes were not thoroughly studied. In this paper, the influences of water at the toe of slopes during shaking were studied using centrifuge modelling technology. Parameters such as the height of water level, relative density, intensity of shaking, and successive shaking were also studied to clarify their influences on the overall stability of slopes.

2. Geotechnical centrifuge and shaking table

The centrifuge model tests were carried out on the shaking table in Kyoto University centrifuge, which has an effective radius of 2.5 m and a maximum capacity of 24 g-ton. The shaking table is integrated with the swing basket of the centrifuge and has a maximum force capacity of 14.7 kN, a maximum acceleration of 50 g, and maximum amplitudes of ± 5.0 mm in the model scale.

Since soil is highly stress dependent and the geotechnical centrifuge can provide an accelerated field of N times Earth's gravity for a model scaled down by $1/N$, results from the tests can be extrapolated to a prototype situation. This is the basic scaling law of centrifuge modelling, that stress similarity is achieved at homologous points by accelerating a model of scale N to N times Earth's gravity. The centrifuge scaling factors were summarized in Table 1.

Table 1 – Centrifuge scaling factors

Parameter	Prototype-model ratio
Length	N
Density	1
Time (dynamic)	N
Time (diffusion)	N^2
Frequency	$1/N$
Stress	1

The rigid container with a slope model in it was fixed onto the shaking table before the centrifuge span up to a centrifugal acceleration field of 50 g. Two consecutive shaking was excited in test 1, 2, 3, 5, and 6, and the intensity of the second shaking was twice larger than that of the first one. The frequency and duration of each shaking were 50 Hz and 0.8 s. In test 4, shaking with a very large intensity was introduced in the shaking table for twice and the frequency and duration were 50 Hz and 0.6 s.

3. Instrumentation

One accelerometer was put at the bottom of the container to record the base acceleration. A high speed camera was mounted in front of the container; the front wall was transparent so that centrifuge models could be viewed and photographed during the tests. At different depths within models, accelerometers were buried

to record the accelerations in different locations. The geometry and instrumentation of each test was shown in Fig. 1.

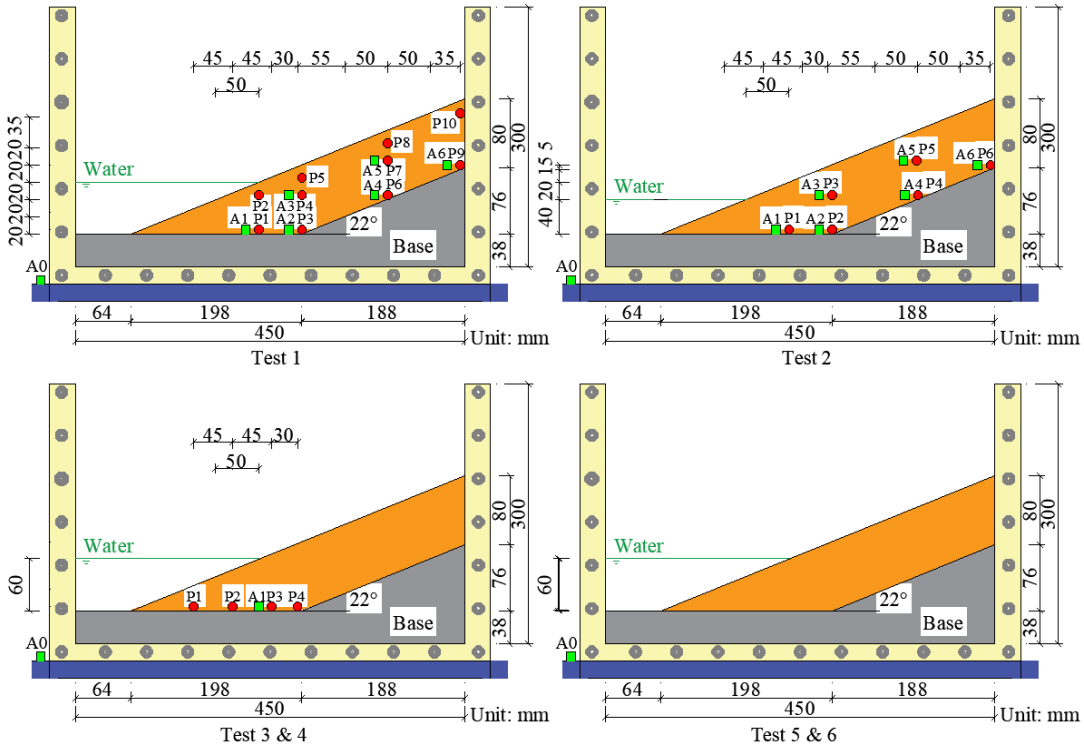

Fig. 1 – Schematic diagrams of geometries and instrumentation in centrifuge models

Several pressure transducers were used to measure the pore water pressures within the models. Before the tests, water was introduced to the designed height in the container.

4. Test progrom

Six tests were conducted on the centrifuge at 50 *g* and the test program was summarized in Table 2. All slope models were rested on a wood base with a slope angle of 22 °and height of 12 cm. And each slope model had the same geometry with a thickness of 6 cm. The base was fixed in the container to ensure its syncing movement with the container when subjected to shaking during the rotation of the centrifuge arm. Then Masado soil was placed and compacted layer by layer with a hammer and the transducers and accelerometers were buried into the soil in this process. The water content of the slope before transferred to the centrifuge was 15% and the soil was initially unsaturated.

Table 2 – Centrifuge model test program

Test No.	1	2	3	4	5	6
Initial water level at base	6 cm	4 cm	6 cm	6 cm	6 cm	6 cm
Relative density	80 %	80 %	70 %	80 %	90 %	80 %

Water was introduced at the toe area of the slope before the specimen was transferred to the centrifuge. The wood base could allow the water to infiltrate along the surface through capillary forces, which provided an easy environment for the soil to move along the inclined base during shaking. Since the soil was unsaturated at the upper part of the slope, it made the slope able to stabilize during the spin-up of the

centrifuge and thus no large soil movement was seen before the slope was subjected to shaking. However, the soil at the lower part of the slope soaked the soil to be soft, which provided a shearing to the slope and allow the soil to travel at high speed.

The relative density of each slope model was achieved by layered compaction. Before the making of slopes, lines were drawn on the inner walls of the container at an interval of 2 cm from the bottom of the base, and the mass of each layer of soil and the water need were calculated before compaction. Each layer of soil was placed after being fully mixed with water and then compacted until it reached its desired line position. The relative density of each layer of soil was thus controlled and thus was the overall relative density of the whole slope model.

5. Test results and discussion

5.1 Deformation of slopes

In the first three tests, a high speed camera was fixed above the container and the tests were filmed. For the last test, the camera was moved to the front so that the plan view photos were not available. Photos of slopes models in first four tests were shown in Fig. 2.

In test 1, massive soil movements didn't occur and the cracks only took place at 2 to 4 cm above the water level. In test 2, due to the lowered water level at the slope bottom, the cracks near the water level were less than those in test 1, even though cracks at the upper part of the slope showed up before shaking during the spin-up process. Shaking-caused cracks only took place in the soil that was near the water level, and the upper part still had good stability,

In test 3, cracks caused by shaking took place at positons closer to the water level and the apertures of them were larger than those in test 1. This was because of the lower stiffness of the slope and the lateral soil displacement was much more. And the cracks at the crest were enlarged and developed, which was not seen in tests 1 and 2. Even though there were some clear cracks on the surface of the upper slope in test 3 during spin-up and before shaking, the shaking-caused cracks were in different locations on the upper slope as well as near water level. This was different from the tests 1 and 2. It also showed that the suction in the soil near water was lowest, and the suction in the middle part of the slope between the cracks was uniformly distributed.

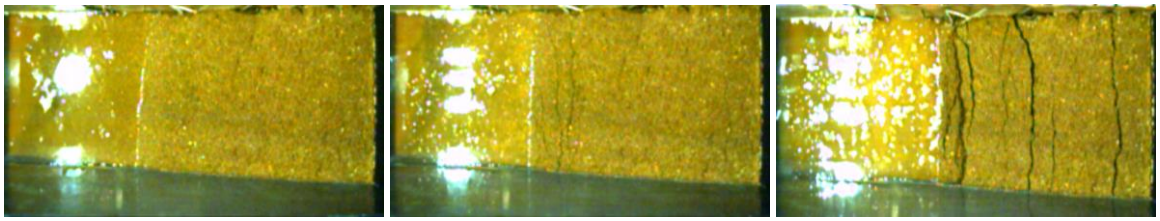

(a) Test 1 (plan view: before and after shaking)

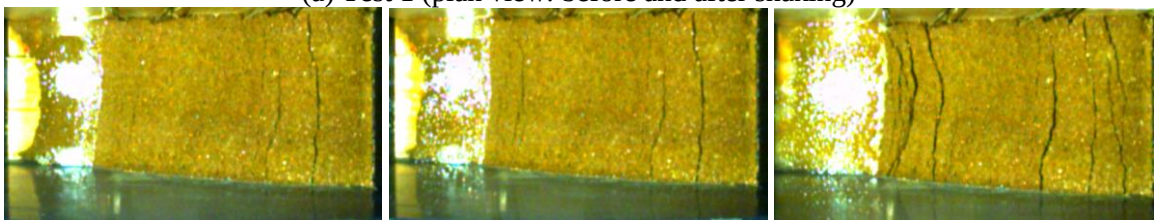

(b) Test 2 (plan view: before and after shaking)

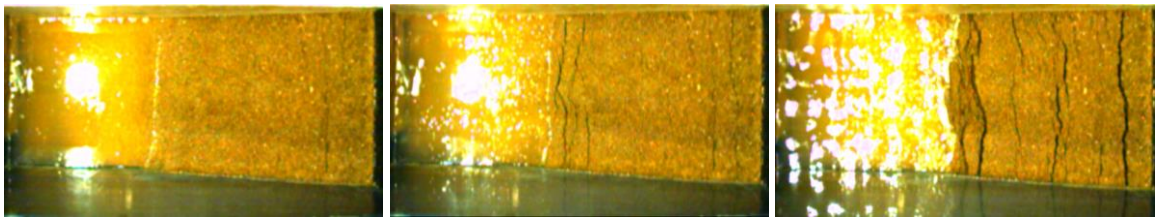

(c) Test 3 (plan view: before and after shaking)

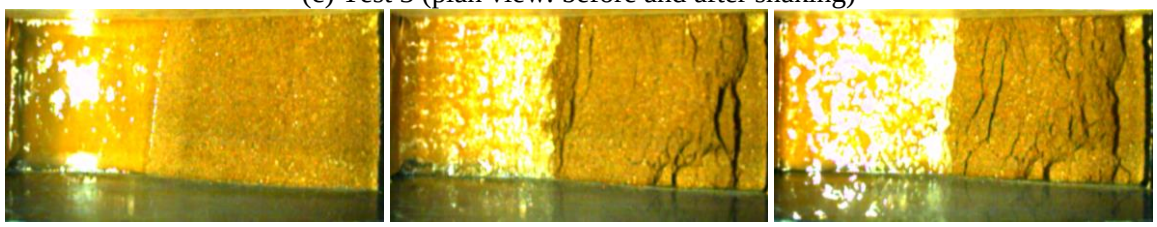

(d) Test 4 (after shaking, elevation and plan views)

Fig. 2 – Slopes after shaking in the tests 1, 2, 3, and 4

In test 4, the shaking was so intense that even the upper slope far away from the water level generated cracks as deep as 6 cm in model scale, as shown in Fig. 2 (d), which was not seen in other three tests. Because of the existing suction in the upper soil, the soil blocks were still stable and no massive soil movement was observed. For the soil few centimeters above the water level, though unsaturated, the water moved upward due to the capillary forces and the soil began settling and moving at very high speed during the intense shaking. The lower slope collapsed, and the settlement and lateral displacement were apparent especially for the soil in the lower section. The soil accumulated at the corner of the container. Failure was associated with long travel distances of soil at lower part of the slope.

5.2 Response of accelerations

Input motions in each test are shown in Figs. 3 and the accelerations and time were in the prototype scale. In tests 1, 2, and 3, slope models were subject to shaking with an amplitude of 1 m/s^2 for 40 s and then shaking with an amplitude of 2 m/s^2 for 40 s (Fig. 3 a and b) and the slope model in test 4 was subject to shaking with an amplitude of 6 m/s^2 for 30 s and then the same shaking for 30 s (Fig. 3 c). In tests 5 and 6, slope models were shaken twice and the amplitudes of the two shaking were about 2 m/s^2 and 4 m/s^2 (Fig. 3 d and e).

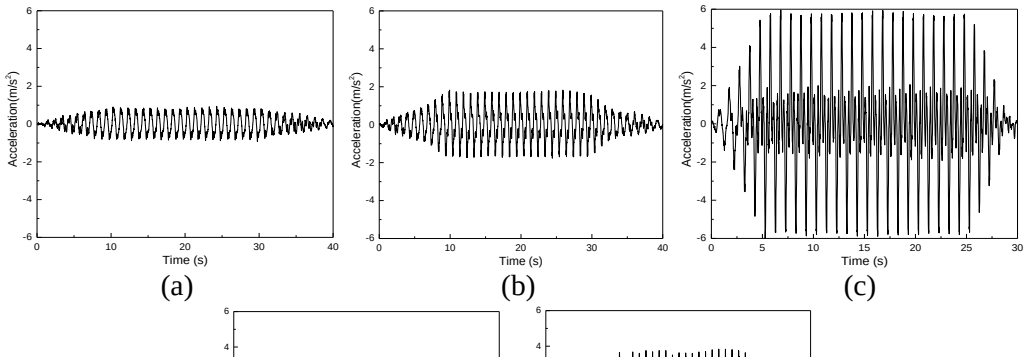

(a) (b) (c)

(d) (e)

Fig. 3 – Input motions: 1st shaking (a) & 2nd shaking (b) in tests 1, 2, and 3; shaking (c) in test 4; 1st shaking (d) and 2nd shaking (e) in tests 5 and 6.

Fig. 4 shows the response of accelerations at various depths of slope models in tests 1, 2, 3, and 4 during the 1st shaking. In tests 1 and 2 the amount of accelerometers were more than those in tests 3 and 4. The geometry and relative density of both tests were the same, the resopnse of accelerations differed though. In test 1, the amplitudes of accelerations in A1, A2, A4, A5, and A6 were larger than input motions except for A3, whose amplitude was the lowest. In test 2, however, A4, A5, and A6 showed larger amplitude increases instead of A1, A2, and A3 with A1 having problematic lowest accelerations. Some accelerometers at the bottom of the slope in each test tilted during shaking, and readings were not zero even after shaking ended. With the omparison between the accelerations of A1 in tests 3 and 4, it could be seen that large sharking resulted in large amplification of soil accelerations at the base.

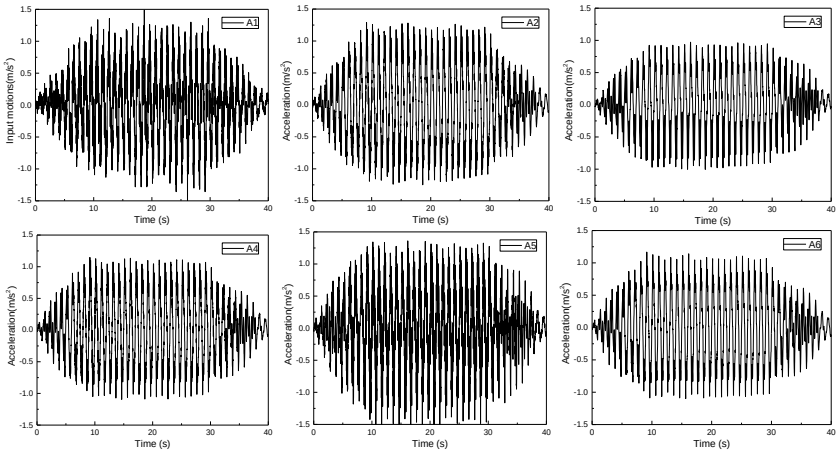

(a) Test 1

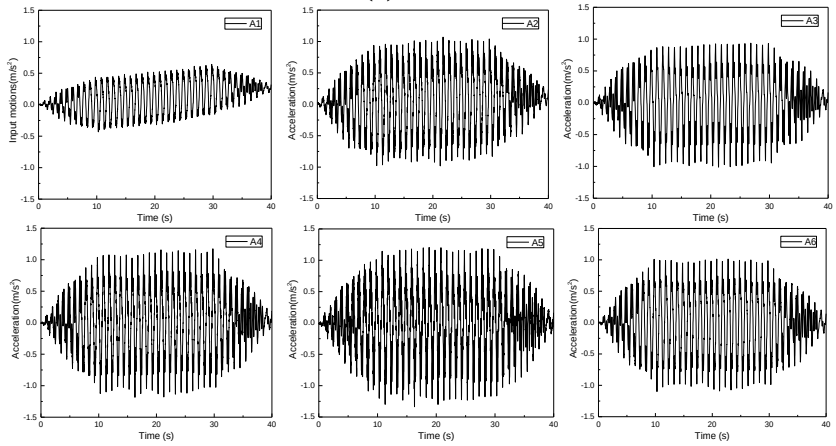

(b) Test 2

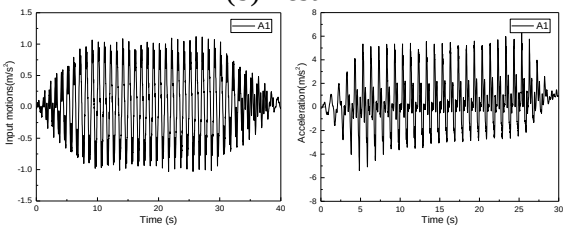

(c) Test 3 (d) Test 4

Fig. 4 – Accelerations in slopes in tests 1, 2, 3, and 4 during 1st shaking.

Fig. 5 shows the response of accelerations at various depths of slope models in tests 1, 2, 3, and 4 during the 2nd shaking. It could be seen that the second shaking caused larger soil movement because the accelerometers (A1, A2, A3, A4, and A5) were tilted, and the soil at the bottom had larger displacement than other parts

since A1 and A2 had more increases in their amplitudes. In test 2, however, it became different and only A3 showed tilt during shaking. A1 in test 3 tilted and A1 in test 4 had larger amplitude during the second shaking. From the response of soil accelerations in the slopes, it was found that the second shaking with a larger intensity than the first shaking induced larger displacement; cracks initiated during the first shaking developed and expanded deeply during the second shaking, which was indicated in Fig. 2,

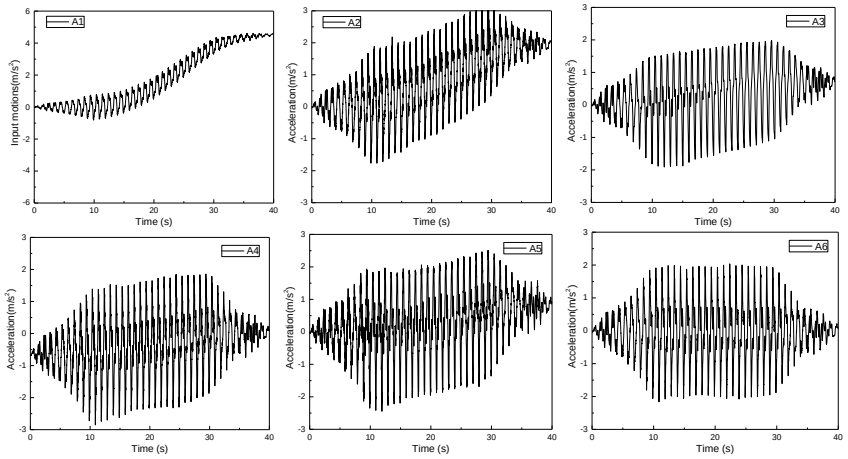

(a) test 1

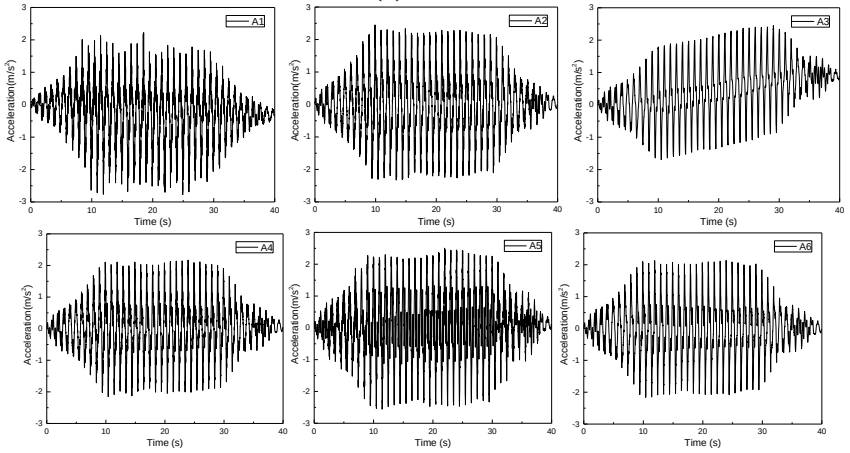

(b) test 2

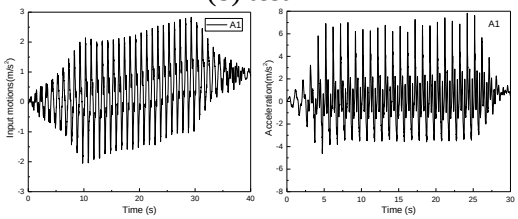

(c) Test 3 (d) Test 4

Fig. 5 – Accelerations in slopes in tests 1, 2, 3, and 4 during 2nd shaking

5.3 Response of pore water pressures

It could be seen in Fig. 6 that, excess pore water pressures were closely related to the shaking intensity. In tests 1, 2, and 3, pore water pressures didn't grow much during small shaking (intensity of 1 m/s^2), but more increases were seen in certain pressure transducers. In test 4, since the shaking intensity was already large enough to cause large excess pore water pressures, the pore water pressures in four transducers were almost in the same trend during the second shaking.

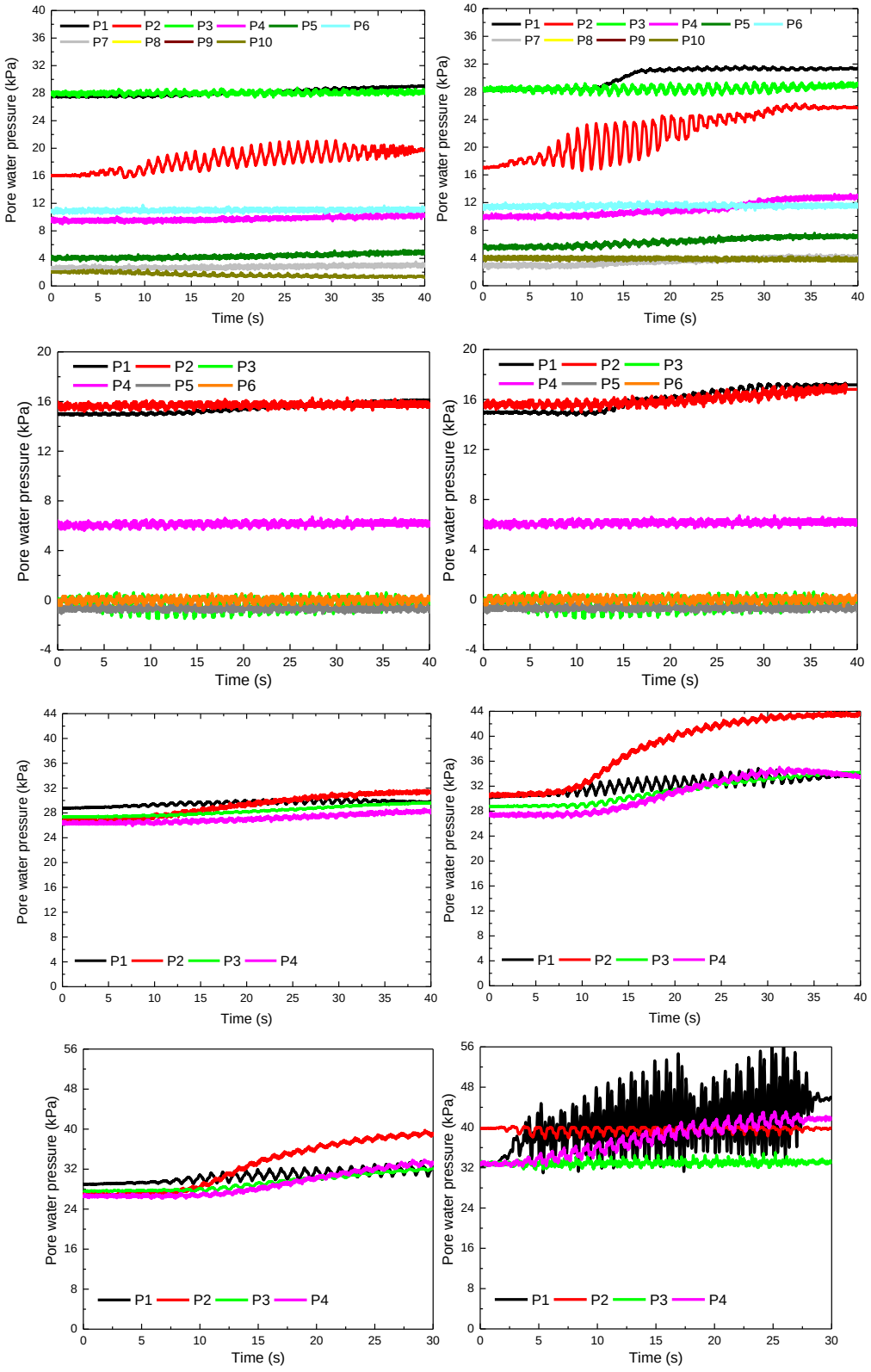

Fig. 6 – Pore water pressures in slopes in tests 1, 2, 3, and 4

In test 1, the water pressures at the base increased especially P1 and P2. No excessive pore water pressures developed at the upper slope, except for the P10 where little suction increased (in Fig. 6). Due to the insufficient infiltration of the water at the toe area, the pore water pressures within the slope were very

small and the shaking was not intense enough to cause large increases in pore water pressures. During the second shaking with a larger intensity, excess pore water pressure developed more in different parts of the slopes. In test 2, because of the low water level at the slope base, excess pore water pressured in didn't develop much. Excessive pore water pressures in P1 rose to 1 kPa, water pressures were negative (suction) but only last to a very limited value (less than 2 kPa) and disappeared at the end of shaking. The suction recorded was not likely to reflect the real conditions in slopes because of the limitation of the transducers used in the tests. In test 3, all four transducers demonstrated increases in excessive pore water pressure and excessive pore water pressures in P2 and P4 were still increasing even after shaking. The relative density of the slope in test 3 was the lowest in all tests, and the all the transducers recorded increasing pore water pressures during shaking. Even though all transducers were in the same level and the depths were the same, the increase in pore water pressures were different, but it showed an increasing trend. In test 4, excessive pore water pressures in four transducers were dramatically higher than those developed in other three tests. Due to the water level increased by the accumulated soil at the bottom, the largest increase in pore water pressure was recorded in P1.

5.4 Displacement

Soil displacement during shaking was obtained from the image analyses of the photos taken by a high speed camera in front of the container. The image analyses were carried out with an image processing software called Dipp Motion. The tracking markers were placed between the front window of the container and the soil while making the specimen by hammer compaction layer by layer. And the calibration markers were also used to calibrate and ensure the accuracy of the analysis results. To check the reliability of the analysis results, the displacement of the calibration markers was used to compare with that of the container; if the two matched each other and had the same amplitude, the analysis was regarded to be accurate. In this way, the analysis results of the tracking markers were ensured to be accurate.

Image analysis results of the soil displacement in slopes in tests 5 and 6 were shown in Figs. 7 and 8, and discussed below. Since only one high speed camera was mounted in front of the container to record the shaking events in tests 5 and 6, the top view of the slopes inflight were not available. However, photos of the slopes in tests 5 and 6 after shaking was taken, and shown in Fig. 9. The input motions in tests 5 and 6 were recorded in Fig. 3 (d) and (e); the first shaking was initiated when the centrifugal acceleration reached 50 g and the second shaking continued as the first one ended.

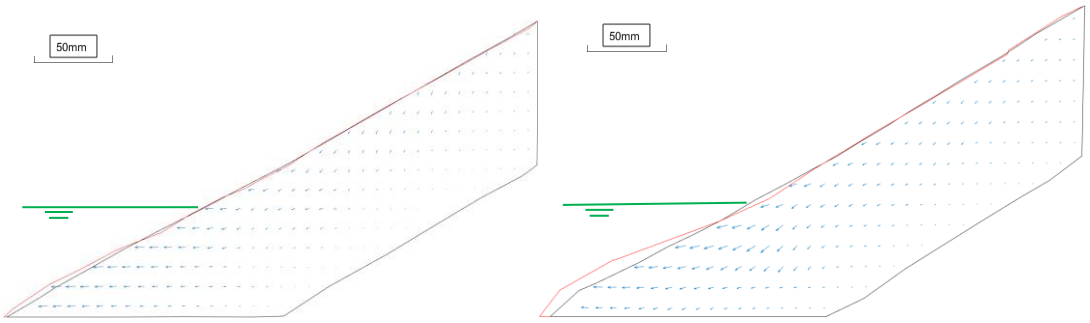

(a) (b)

Fig. 7 – Displacement of model slope in test 5: first shaking (a) and second shaking (b)

In the first shaking, the slope didn't generate much displacement on the upper part, but the soil movement below the water level were mainly horizontal, which could be seen in Figs. 7 (a) and 7 (b). This was because the soft soil below water level tended to move easily during shaking.

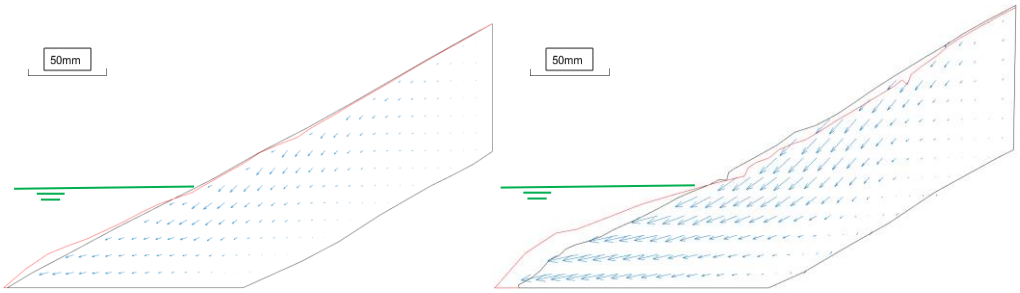

(a) (b)

Fig. 8 – Displacement of model slope in test 6: first shaking (a) and second shaking (b).

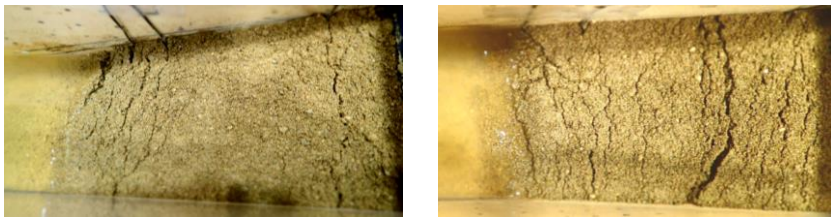

(a) (b)

Fig. 9 – Top views of the model slopes in tests 5 and 6 after the second shaking

Horizontal displacement of the soil on the lower part made the soil on the upper part unstable and displacement occurred. When the second shaking with a much larger intensity than the first one came, the displacement of soil especially on the lower part was much larger, leaving cracks on the surface of the upper slope. The displacement in Fig. 8 (a) were larger than that in Fig. 7 (a) especially in the area near the water level, and the maximum displacement after the first shaking in both slopes were 0.98 mm and 3.2 mm in the model scale.

When the second shaking came, the displacement continued to develop and the soil below water had the largest movement in both tests (Figs. 7 (b) and 8 (b)). Soil slid and accumulated at the bottom of the slopes after the shaking ended. The cracks in the slope in test 5 after shaking were relatively shallow. The largest depths of the cracks in slope in test 6 were about 1 cm in model scale. From the top views in Fig. 9, the characteristics of the shaking-induced cracks could be seen clearly. The cracks in slope in test 5 concentrated on the surface of the soil within 10 cm above the water level, and the middle part of the slope didn't have clear cracks except one crack on the top. However, cracks in the slope in test 6 distributed on the whole slope surface with one obvious and deep crack on the upper middle part of the slope. The wide and deep crack was induced by the large soil movement in the lower part of the slope. Cracks were also found on the surface of the middle part of the slope, which were quite different from those in the slope in test 5.

With a larger soil relative intensity, the slope in test 5 didn't generate as much displacement as in the slope in test 6. The outline of the slope in test 6 was almost 1 cm in model scale lower compared to its original outline before shaking, and had more cracks on soil above the water level after the second shaking than the slope in test 5. The direction of the tensors around the water level was almost parallel to the inclined base while the direction of the tensors at the toe area in the slopes were almost horizontal. The largest displacement in the slope in test 6 was 29.1 mm, while the largest displacement in the slope in test 5 was only 10.9 mm in model scale.

For the slope above the water level, the further the soil was from the water level, the smaller the displacement was; the deeper the soil, the smaller the displacement was. In the upper and deep soil in the slopes in Figs. 7 (b) and 8 (b), the displacement was much smaller than that in the lower parts of the slopes. This was because the capillarity in the soil near the inclined base and far from the water level was not

significant, suction in the soil near the base was high and so was the shear strength. Infiltration of water into the soil was mainly few centimeters below the surface, and the loss of suction in the soil resulted in large soil displacement. If the time for water infiltration was longer, the displacement in the deep soil would be larger and the slope would be more mobilized, causing a large sliding area, as well as wider and deeper cracks.

6 CONCLUSIONS

In the centrifuge model tests carried out in this study, the water at the bottom of the slope had a great influence on the slope stability. When slopes were subjected to water storage at the toe area, the soil below and right above water level tended to be compressible and loose, and the slope behavior became different compared with those without storage.

The compression of the soil below the water level and localized failure at the toe region acted as the main trigger to shear the soil located away from the water level. Because of widely existing high suctions in the upper part of the slopes, total collapse was not possible even in model where intense shaking was excited. Seepage and capillary flow are two factors that need further attention in the study of the dynamic response of slopes subjected to water storage at toe. Cracks were concentrated at areas near the water level. Increasing the shaking intensity or successive shaking on a slope with a certain height of water at its toe area will not produce total collapse of the slope unless more infiltration time is given before the shaking. A large landslide below certain height of the slope can be caused by a strong shaking and the cracks on the unsaturated part of the slope is deepened as the intensity of the shaking increases.

The shaking in tests in this study was introduced right after designated centrifugal accelerations were achieved and the time for seepage and capillary rise was very limited. In future study, model tests with elongated time for these phenomena are needed.

7. References

[1] Fujita H (1977): Influence of water level fluctuations in a reservoir on slope stability. *Bulletin of the International Association of Engineering Geology*, **16** (1), 170-173.

[2] Kilburm CR and Petley DN (2003): Forecasting giant, catastrophic slope collapse: lessons from Vajont, Northern Italy. *Geomorphology*, **54** (1), 21-32.

[3] Miao F, Wu Y, Li L, Tang H, Li Y (2018): Centrifuge model test on the retrogressive landslide subjected to reservoir water level fluctuation, *Engineering Geology*, **245**, 169-179.

[4] Pinyol NM, Corominas J, Moya J (2012): Canelles landslide: modelling rapid drawdown and fast potential sliding. *Landslides*, **9** (1), 33-51.

[5] Qi S, Yan F, Wang S, Xu R (2006): Characteristics, mechanism and development tendency of deformation of Maoping landslide after commission of Geheyan reservoir on the Qingjiang River, Hubei Province, China. *Engineering Geology*, **86**, 37-51.

[6] Sun GH, Zheng H, Tang HM, Dai FC (2016): Huangtupo landslide stability under water level fluctuations of the Three Gorges Reservoir. *Landslides*, **13** (5), 1167-1179.

[7] Wang H, Xu W, Xu R, Jiang QH, Liu JH (2007): Hazard assessment by 3d stability analysis of landslides due to reservoir impounding. *Landslides*, **4** (4), 381-388.

[8] Wang JE, Xiang W, Lu N (2014): Landsliding triggered by reservoir operation: a general conceptual model with a case study at Three Gorges Reservoir. *Acta Geotech*, **9** (5), 771-788.

[9] Xiong X, Shi Z, Xiong Y, Peng M, Ma X, Zhang F (2019): Unsaturated slope stability around the Three Gorges Reservoir under various combinations of rainfall and water level fluctuation. *Engineering Geology*, **261**, 1-17.

